Observations and EOF Analysis of Low-Frequency Variability in the Western Part of the Gulf Stream Recirculation†

ANGELIKA LIPPERT* AND MELBOURNE G. BRISCOE**

Woods Hole Oceanographic Institution, Woods Hole, Massachusetts

(Manuscript received 17 August 1987, in final form 3 November 1989)

ABSTRACT

This study of low-frequency oceanic variability is based on data collected during the Long Term Upper Ocean Study (LOTUS), which was a two year program of (mainly) moored meteorological and oceanographic measurements. The mooring arrays were centered at 34°N, 70°W over the Hatteras Abyssal Plain. With a distance of about 300 km to the mean Gulf Stream axis and the continental slope, LOTUS was the most northern and western long-term mooring site in the Gulf Stream recirculation region to date.

The observed low-frequency variability is dominated by zonally elongated motions of the secular time scale (periods > 100 days) even at great depths (4000 m). In contrast to observations in other parts of the recirculation region, the spectral shapes are strongly depth dependent.

The vertical structure of the variability was examined by EOF analysis. Different kinds of EOFs were tested; the best representation of the observed variability was obtained by an EOF representing a unidirectional nonrotating (with depth) flow. The first and second EOF together explain 96% of the observed energy. The first EOF (66%) is almost barotropic with a slight increase at the surface and the bottom of the ocean; the second mode closely resembles the first baroclinic dynamical mode. The barotropicity decreases with increasing frequency. Motions with periods less than 30 days are almost surface trapped, and a strong bottom intensification additionally exists for periods between 10 and 30 days.

The low-frequency flow at LOTUS is consistent with a stochastic, quasi-geostrophic wave field that may be affected by a mean current, but our observations are insufficient to test this hypothesis.

1. Introduction

During the last two decades the low-frequency oceanic variability in the western North Atlantic has been extensively examined in several large experiments as part of MODE (e.g., MODE Group 1978; Fu et al. 1982) and POLYMODE (e.g., Mills et al. 1981; McWilliams et al. 1983). Emphasis was placed on the interaction of the eddies with the mean circulation and on the sources for the eddies.

A dominant property of the eddy field in the western North Atlantic is its large-scale spatial variability. A prominent feature of the horizontal structure is the correspondence of the kinetic energy of the mean current with the surface eddy kinetic energy (Wyrtki et al. 1976; Richardson 1983; Schmitz et al. 1983) as well as with the abyssal (4000 m) eddy kinetic energy (Schmitz 1976, 1984).

The vertical structure and the shape of the spectra also change geographically (Richman et al. 1977; Fu et al. 1982; Schmitz 1978; Wunsch 1981). Explanations for the horizontal inhomogeneity of the spectra require more factors than just the geographical changes of the mean kinetic energy. The general tendency along 70°W for a relative shift in energy toward higher frequencies as one progresses northward has been suggested, for instance, as being related to the bottom slope (Schmitz 1974; Luyten 1977; Schmitz 1978); horizontal changes of the wind field or vertical shear of the mean current have not yet been considered.

Due in part to the similarity in the patterns of the maximum kinetic energy and the mean current, the main source of the eddy field has been thought to lie in the baroclinic and barotropic instability of the mean current. Wind forcing is thought to be a possible source only for low-frequency variability in the central oceans (Müller and Frankignoul 1981), because the energy level of linear quasi-geostrophic motions forced by stochastic wind is thought to be much smaller than the energy levels observed near the Gulf Stream. However, a quantitative assessment of the role of wind forcing in the recirculation region has not been done because of the lack of simultaneous long-term space–time

† Woods Hole Oceanographic Institution Contribution Number 6872.

* Present affiliation: Institut für Meereskunde an der Universitat Hamburg, Hamburg, Federal Republic of Germany.

** Present affiliation: Office of Naval Research, Arlington, Virginia.

Corresponding author address: Dr. M. G. Briscoe, Office of Naval Research, Code 124, 800 North Quincy Street, Arlington, VA 22217-5000.

measurements of the relevant oceanic and atmospheric quantities.

The *Long Term Upper-Ocean Study*, subsequently referred to as LOTUS, provided new data for examination of the horizontal inhomogeneity of the eddy field as well as the sources of the eddies. LOTUS was a two-year program of meteorological and oceanographic measurements mainly based on moorings. The moorings were situated near 34°N, 70°W over relatively smooth bottom topography in the deep water of the Hatteras Abyssal Plain. With only 300 km distance to the mean axis of the Gulf Stream and to the major continental slope, LOTUS was the most northern and western long-term mooring site in the Gulf Stream recirculation region to date (Fig. 1). In this region the mean currents are historically weak, but the eddy activity is strong. Local sources such as baroclinic instability of the mean current or wind forcing as well as remote forcing through westward propagating Rossby waves or Gulf Stream rings could all cause the low-frequency variability in this region.

The LOTUS scientific design emphasized the role of atmospheric forcing not only for the eddy variability but for a variety of other oceanic motions having periods between a few hours and several months; see Price et al. (1987) for one such result. In addition, a goal was the determination of the variability and energetics of the internal wave field over several seasons and under different environmental situations such as in the presence of Gulf Stream rings or near oceanic fronts. A detailed description of the experiment is given in Woods Hole Oceanographic Institution technical reports (Trask et al. 1982, 1983a,b,c; Deser et al. 1983; Montgomery et al. 1984a,b; Tarbell et al. 1984, 1985).

Preliminary results of LOTUS based on the first year of the mooring measurements were presented by Briscoe and Weller (1984), who classified the variability into high frequency, inertial and low-frequency variability. According to this classification we discuss here the low-frequency part of the variability covering phenomena with periods between 2 days and 717 days. We have available a nearly continuous time series of 717 days length for the wind stress components, the velocity components at seven depths and temperature at five depths as shown in Fig. 2. A 24-hour gaussian-filtered, daily-averaged version of the data is the basis for these low-frequency variability studies. In this paper only the more descriptive parts will be presented, i.e., the typical time scales (section 1) and vertical scales (section 2).

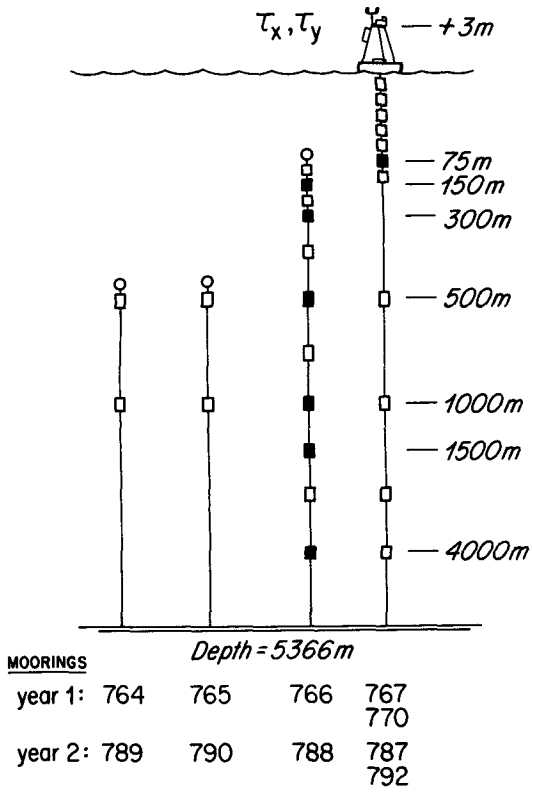

FIG. 2. Schematic of the LOTUS moorings, showing current meters (open rectangles) from 5 m to 4000 m on intermediate (left two moorings), near-surface, and surface moorings. Those depths and mooring types used here are shown as black rectangles; all instruments used were Vector Averaging Current Meters (VACM) except at 75 m, where a Vector Measuring Current Meter (VMCM) was used. All instruments used gave velocity and temperature records except those at 75 and 4000 m, which provided velocity only. See Tarbell et al. (1984, 1985) for mooring and instrument details; the relevant mooring numbers are given at the bottom of the figure.

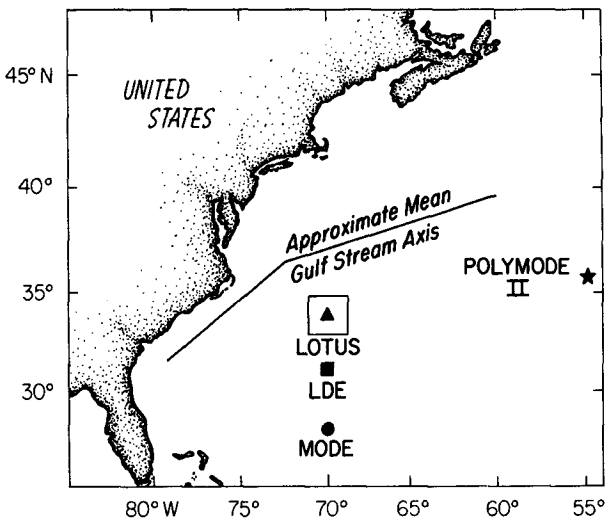

FIG. 1. Location of the LOTUS area and the locations of other long-term mooring sites.

2. Time scales

Spectral analyses were performed for time series of the velocity components at those seven depths where the two-year record was available. They are presented here as log/log plots of the kinetic energy at different

depths (Fig. 3a), as decadal (energy- or area-preserving) kinetic energy spectra in Fig. 3b to permit comparisons with results of other long term measurements (Schmitz 1978; Owens 1985) and as a special kind of decadal depth-integrated spectrum of the velocity components (Fig. 4).

In Fig. 3a, in which the energy-density spectra at four different depths are presented (150 m, 500 m, 1000 m and 4000 m), the red spectral nature of the kinetic energy is obvious. The energy level decreases slightly with increasing depth but increases again near the bottom; thus, the 4000 m energy level is larger than that at 1000 m. The spectra do not show any significant peaks, and drop off smoothly with increasing frequency. At 150 and 500 m the spectrum drops off as about $(\text{freq})^{-2}$, which also corresponds to predictions of linear quasigeostrophic models (Müller and Frankignoul 1981; Lippert and Kase 1985) for the first baroclinic mode. At 1000 m and deeper the spectrum drops off as $(\text{freq})^{-2.5}$ and steeper.

Schmitz (1978) compared the observed low frequency variability at the MODE CENTER region (28°N, 70°W) with that observed near the Gulf Stream during POLYMODE II (mooring PM08: 37.5°N, 55°W) by means of decadal kinetic energy spectra. He showed that near the Gulf Stream (POLYMODE II) the shape of the spectrum is almost depth independent and is dominated by a peak at the temporal mesoscales (periods of 60–100 days). In the MODE area the temporal mesoscale is prominent only at abyssal depths (4000 m) while it is almost completely masked in the thermocline by even lower-frequency energy (secular scale, which has periods > 100 days). Recent results on low-frequency variability at the Local Dynamics Experiment (LDE; 31°N, 70°W) (Owens et al. 1982; Owens 1985) show frequency spectra dominated by the secular scale and a peak in the period range between 30–60 days. The shape of the spectra is not strongly depth dependent there, either.

The LOTUS results (Fig. 3) do not support any clear tendency in the evolution of the shape of the spectra from south to north along 70°W and to the PM08 mooring site near the Gulf Stream extension. Shown in Fig. 3b are the decadal frequency spectra at 4 depths (150 m, 500 m, 1000 m and 4000 m). Their shapes change from depth to depth much more than in other regions with strong mean currents (LDE, POLYMODE) but less so than at MODE, which had weak mean currents. The shape at 150 m shows similarities to that found during LDE at 500 m, but even at this depth the secular scale dominates the variability; it contains 40% of the energy compared to 12% in the mesoscale and 18% in the period range of 30–60 days. The secular scale becomes important with greater depth (it contains 56% of the energy at 4000 m); the mesoscale loses importance with depth and the percentage of energy contained in the 30–60 day period range stays about constant. A detail to be noted in this figure is

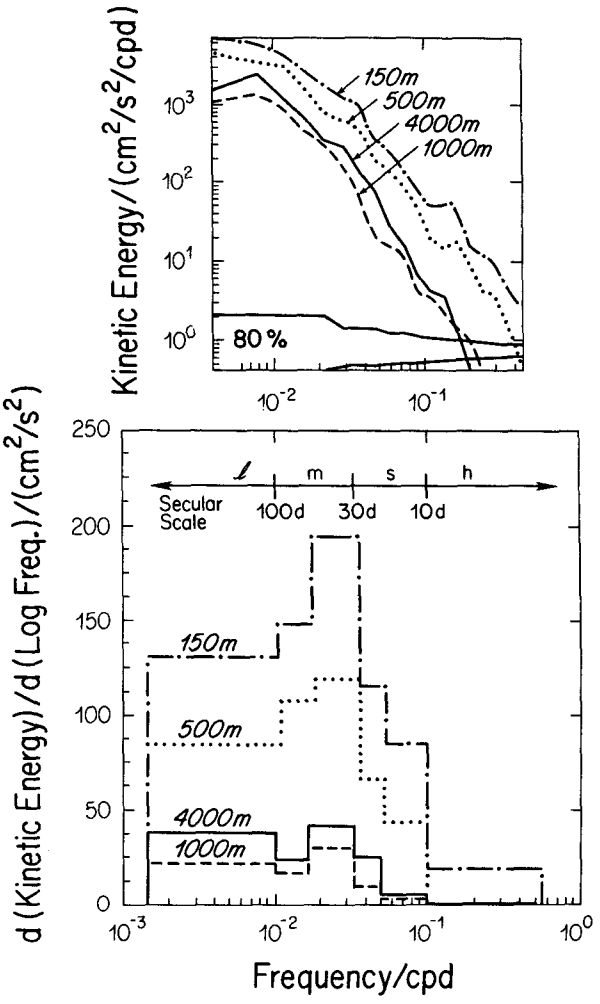

FIG. 3. (a) (top) Kinetic energy spectra at 150 m depth (dashed line with dots), 500 m depth (dotted line), 1000 m depth (dashed line) and 4000 m depth (solid line). (b) (bottom) Decadal kinetic energy spectra at the same depths as in (a). The scale along the top shows the secular and mesoscale ranges, and the coding used in Fig. 4.

that, while the percentage of energy at all period ranges < 30 days decreases from the top of the ocean to the thermocline and the decrease continues for periods < 20 days for greater depths, the percentage of the energy contained in periods *between* 20–30 days *increases* at greater depths. Evidence for this feature, which is possibly connected with topographic waves, is also given in the empirical eigenfunctions of the energy-weighted cospectral matrix for the 10–30 day period range (section 2, Fig. 10).

To demonstrate how each velocity component contributes to the kinetic energy, we prepared a decadal, area-preserving, vertical presentation of the kinetic energy (Fig. 4). The whole shaded area corresponds to 100% of the observed depth-integrated kinetic energy. Each area with a different shading, divided from the others by a solid line, corresponds to the fraction of

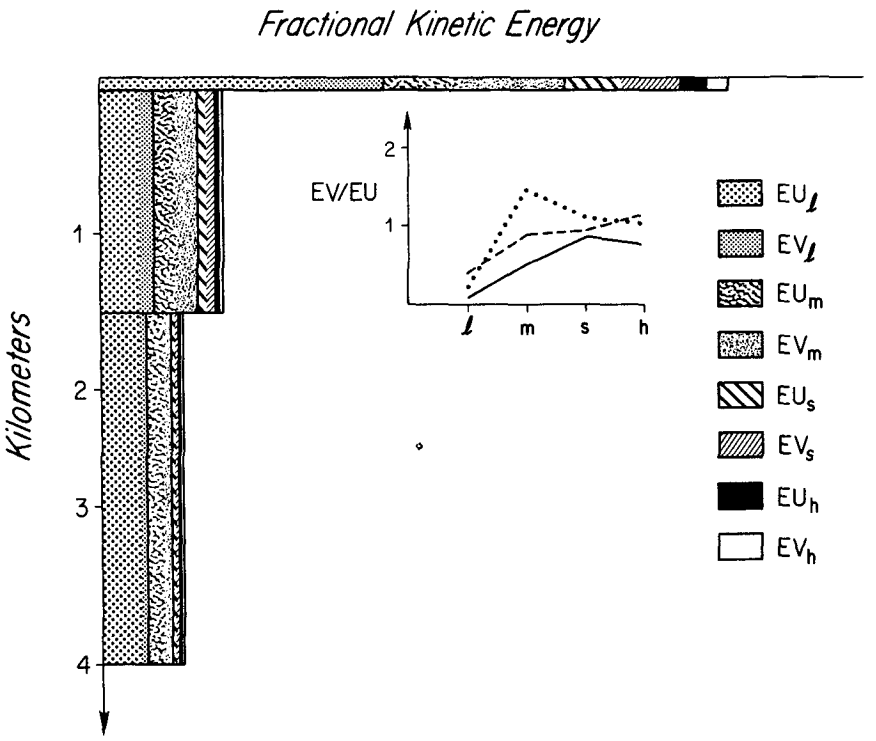

FIG. 4. Fraction of kinetic energy contained in various frequency and depth ranges (shaded area plotted to the left) and the ratio of the energy of the meridional and zonal velocity components (inset small figure). The whole shaded area corresponds to 100% of the kinetic energy. The subscripts correspond to

ℓ low frequency range (periods: >100 days)
m medium frequency range (period: 30–100 days)
s special frequency range (periods: 10–30 days)
h high frequency range (periods: <10 days).

Inset figure to the right: The dotted curve corresponds to the values in the upper-most depth range (0–75 m); the dashed line corresponds to the medium depth range (down to 1500 m); the solid line corresponds to the lower ocean.

the kinetic energy integrated over the corresponding depth and frequency range. Within each kind of depth–frequency bin the zonal and meridional velocity component are distinguished by coarse/fine patterns where the coarser-grained pattern corresponds to the zonal velocity component. The breadth of each patterned area is a relative measure for the energy of each velocity component averaged over the particular depth interval. We chose four different period ranges (see also Fig. 3b) for this presentation. The "low frequency" part (subscript ℓ) covers the secular scales of our observations (periods between 100–717 days). The 30–100 day medium frequency range (m) encompasses the 60–100 day mesoscale defined by Schmitz et al. (1983) and the 30–60 day range. In addition, we define a "special" range (s) for periods between 10–30 days because at these periods the EOFs will show bottom intensification consistent with topographic Rossby waves, and the period range is bounded by the mesoscale on the long-period side and by linear resonant barotropic Rossby waves on the short-period side. Finally, there is the high frequency (h) range (2–10 days).

The total depth interval is divided into three different depth ranges. The first interval corresponds to the uppermost 75 m including from the theoretical point of view the option of quasi-geostrophic and ageostrophic motions. The middle interval includes the main thermocline (75–1500 m) and the third depth interval covers the deep ocean. This kind of grouping is also chosen because the same three depth intervals are meaningful for vertical EOFs discussed subsequently since temperature and velocity time series are complete only for the middle depth range.

Figure 4 shows that the zonal velocity at the secular scales (EU$_\ell$) is the largest single component of all the low frequency variability. Even in the deep ocean about half of the kinetic energy comes from the zonal velocity component in the lowest frequency band. In addition, it is remarkable that the zonal velocity at the secular scales is almost barotropic below the surface layer. The

importance of the zonal velocity component for the kinetic energy, however, decreases with increasing frequency. In the mesoscale frequency range the contribution of the meridional velocity component to the kinetic energy dominates in the uppermost depth interval, and in middle depths is about the same as that of the zonal velocity component. In the deep ocean the zonal velocity component still dominates. At higher frequencies, where the contribution of the zonal and meridional velocity components is about the same, their contribution to the total kinetic energy is quite small.

Although we observe no correspondence between the shape of the low-frequency spectra and the energy level that is definitely related to the distance to the Gulf Stream (Richardson 1983; Schmitz 1984), we suggest the following synthesis based on the low-frequency variability results of Schmitz (1978), Owens et al. (1982), Owens (1985), and these results from LOTUS.

The energy at secular scales *in the thermocline* is the same at the MODE and LDE mooring sites. In the recirculation region (LOTUS, POLYMODE) the energy in this period range is twice the energy of the secular scale at MODE. This small increase from south to north might be related to the increase of the rms amplitude of the wind field (Willebrand 1978) rather than to the increase of the mean current (Wyrtki et al. 1976); we cannot tell. Nevertheless, the importance of the secular scale for the entire range of low-frequency variability *measured as a percentage of the total kinetic energy* is strongly dependent on the energy at the mesoscale. The temporal mesoscale energy and variability in the 30–60 day period band also increases as the Gulf Stream is approached, but the increase is much stronger than in the secular band. The energy of the secular scale *at the 4000 m level* changes horizontally in about the same way as at the 500 m level, but only at LOTUS does the secular scale account for most of the energy observed at 4000 m (56%). At this depth the energy contained in the mesoscale and in the period range from 30–60 days is the same as observed at LDE, which is much smaller than at POLYMODE and larger than at MODE. Thus, more factors than the distance to the Gulf Stream are required to explain the spatial inhomogeneity of the low-frequency spectra. Spatial inhomogeneity of the vertical shear of the mean current and of deep mean currents on bottom slopes could be possible factors; neither can be quantified well with LOTUS data.

The zonally elongated motions (which were also found in the thermocline at MODE, Richman et al. 1977) and the almost barotropic structure at LOTUS (Fig. 3, see also the next section) are characteristics of quasi-geostrophic turbulence (Rhines 1975, 1977), in which energy in the barotropic mode will tend to cascade to low zonal wavenumbers. Zonal elongation is also a prominent feature of linear Rossby waves in a certain frequency range (Lippert and Kase 1985). However, a strong horizontal anisotropy of the velocity field, as observed at LOTUS, which can be measured by the ratio of the energy of the meridional velocity component to the zonal velocity component (EV/EU; Fig. 4, small inset), can only be found in models of linear Rossby waves if the forcing shows the same anisotropy (Lippert and Kase 1985); this kind of anisotropy has not been found in the stochastic component of the wind field. On the other hand, primarily wind-forced Rossby waves secondarily amplified by baroclinic instability of a mean shear flow (which does not have to have very large amplitudes) can also lead to zonal bands (Lippert 1986).

3. Vertical structure

To examine the vertical structure of the observed variability in more detail, the empirical orthogonal function (EOF) technique is used. The simplest EOFs are determined as the eigenfunctions either of (i) the average covariance matrix of a real or complex scalar (Moore 1974) or (ii) the average cospectral matrix of the Fourier transform of the corresponding scalar (Wallace and Dickinson 1972). The scalar can be either the temperature or one of the velocity components (Kundu et al. 1975).

To get the characteristic vertical structure of a vector quantity like the velocity field, we either have to incorporate the velocity components as independent scalar quantities (the dimension of the covariance matrix is doubled to twice the number of instrument depths) or to combine the velocity components in some way into a single quantity. One way to reduce the velocity covariance matrix to one of a single scalar is by calculating the covariance matrix as the dot product between the velocities (Davis 1975). In this case, the observed velocity field is represented by a unidirectional flow for which only the amplitude is allowed to change with depth. Another possibility lies in a complex representation of the velocity field:

$$U = u + iv.$$

In this case the desired eigenfunctions are, in addition, allowed to veer with depth (Kundu and Allen 1976; Hardy 1977; Hardy and Walton 1978; Legler 1983; Denbo and Allen 1984; Klink 1985). Each of the possible kinds of velocity covariance matrices corresponds to a specific model idea about the velocity field, whereby the most general (i.e., least constrained) approach is given by considering the velocity components as independent quantities.

Finally, information about the statistical relationship between the temperature and the velocity field can be found from the EOFs of the covariance matrix calculated by assuming that u, v and T are independent scalars (Owens 1985; Hogg 1985).

Owens (1985) presented a comprehensive meth-

odology of calculating vertical EOFs and suggested comparing the different EOFs to get some information about the dynamics of the observed variability. We will follow his approach to make our results directly comparable to his results about the low frequency variability at the LDE mooring site, which was situated 300 km south of the LOTUS mooring site.

Owens used covariance matrices that, in addition to weighting with the variance at each instrument, were also weighted with the depth intervals between the instrument depths. Thus, his EOFs gave the best representation for the depth-integrated energy; we call these EOFEs. We will, in addition, consider the EOFs of only the variance-weighted covariance matrix (EOFV, here) and compare them with the EOFEs. The different kinds of weighting can lead to different EOFs if the measurements are not vertically equidistant, as in LOTUS. Which kind of weighting is preferable depends on the application, as in most statistical methods.

We begin by considering the modes resulting from the most compressed representation: the dot-product velocity. The first two EOFs represent 94% (variance weighting) or 96% (energy weighting) of the observed variability in the velocity field. However, the EOFs of the variance-weighted covariance matrix (EOFV) are quite different from those of the depth-integrated energy-weighted covariance matrix (cf. Owens 1985), referred to here as EOFE. The first EOFV (Fig. 5a), which shows a decrease in the uppermost 1000 m but stays constant below 1000 m, represents 85% of the observed variability; the second mode (5b), which describes the observed bottom intensification, represents only 8%. In the case of the energy-weighted covariance matrix, more importance is attached to the observed bottom intensification, thus the first EOFE (5c) (66%) shows an increase at greater depths but generally has a weaker depth dependency than the first EOFV. Twenty-nine percent of the variability is described by the second EOFE (5d), which closely resembles the first baroclinic dynamical mode (Fig. 6b).

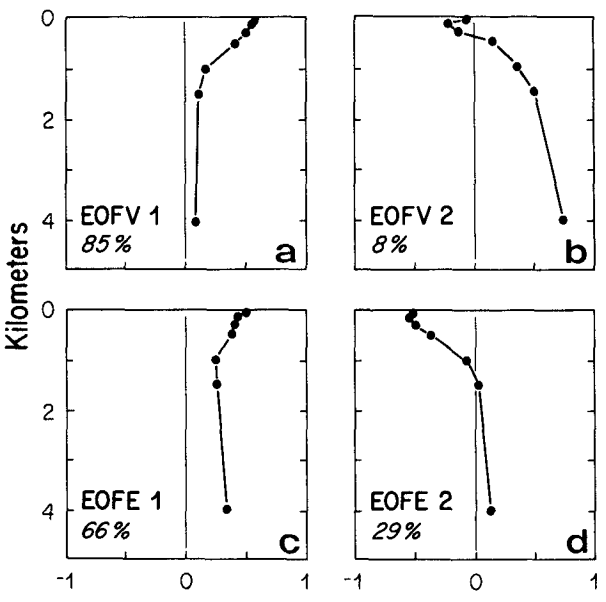

FIG. 5. First and second EOFV and EOFE, which are obtained from the covariance matrix of the time-averaged, velocity dot-products. Panels a and b show the EOFVs obtained from the variance-weighted covariance matrix. Panels c and d show the EOFEs, for which the covariance matrix is weighted proportionally to the separation between instruments.

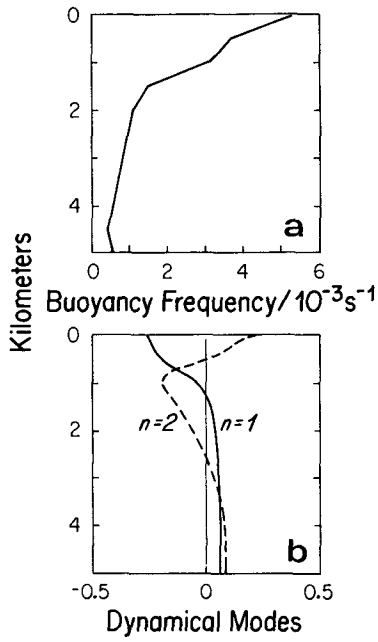

FIG. 6. (a) Vertical profile of the mean buoyancy (Brunt-Vaisala) frequency obtained from the Levitus dataset (1982) and, (b) the first and second baroclinic dynamical modes. The Rossby radii are 33.5 and 14.5 km, respectively.

With the exception of the second EOFV, the EOFs can be reasonably well described by a linear superposition of the barotropic and first baroclinic dynamical modes. Near the surface additional dynamical modes are necessary to describe the shape of the EOFs; this suggests a stronger cross-modal coupling (McWilliams et al. 1986) near the surface. It is remarkable that the ratio of the barotropic and first baroclinic mode is about 1 to 1 for the EOFVs while the first EOFE is dominated by the barotropic component (ratio 11 to 1) and the second EOFE by the first baroclinic mode (ratio 1 to 9).

For comparisons of vertical EOFs of the low-frequency variability at different locations, it is therefore necessary to compare the same kind of EOFs. In Fig. 7 the EOFEs of LOTUS, LDE (Owens 1985) and MODE (after Davis 1975) are presented. *The barotropicity of the observed variability (in the sum of the first two EOFs) increases from south to north,* which is supported by the ratio of the barotropic to the first baroclinic mode of the first EOFE which is about 1 to 1 at

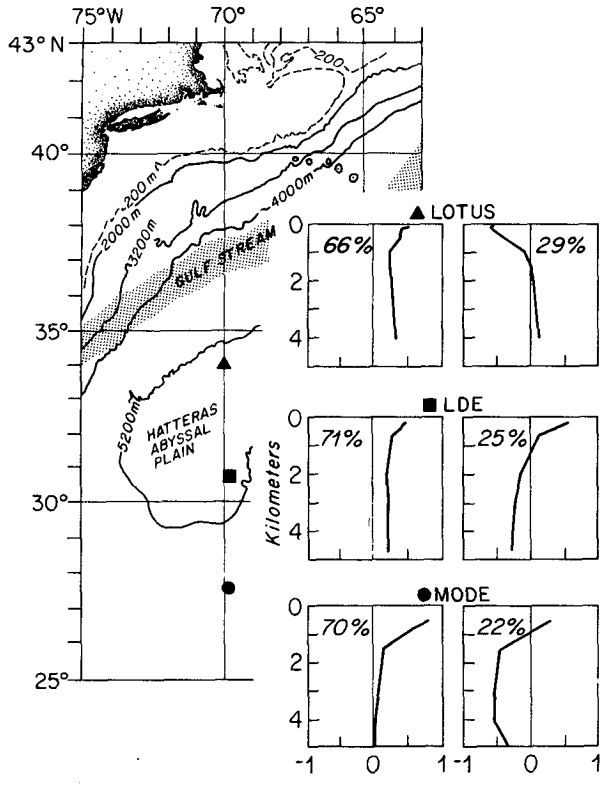

FIG. 7. First and second EOFEs of LOTUS (triangle), LDE (square), and MODE (circle).

MODE, 3 to 1 at LDE (Owens 1985) and 11 to 1 at LOTUS. The increase of the barotropicity from south to north is accompanied by a *decrease of the surface intensification and a small increase in the bottom intensification.* Note that all three sites are on the Hatteras Abyssal Plain and are quite far from the continental slope; LOTUS is closest, at about 300 km. Also at the POLYMODE II mooring site (36°N, 55°W) even the low frequency variability with periods greater than 100 days was found to be predominantly barotropic (Hogg 1985; Schmitz 1978). As Schmitz (1978) pointed out, by comparing the vertical structure of the kinetic energy at POLYMODE II and the MODE mooring site (28°N, 70°W), the increase of the barotropicity seems to be related to an increase in the energy level, which would support general theoretical arguments of Rhines (1977). These results from LDE and LOTUS further support the hypothesized relation between the barotropicity and the energy level.

The next less constraining EOF case (Owens 1985) is the veering modes resulting from the time-averaged covariance matrix of a complex combination of the velocity components (see above). These EOFs turned out to resemble the EOFs of the velocity dot-product covariance-matrix (Fig. 5) in all details, and therefore are not shown. The corresponding phases, which describe the depth-veering from the velocity direction at the surface, are small and statistically not different from zero. This indicates that the average quadrature cross spectrum of the velocity components is zero, which is in agreement with linear quasi-geostrophic wave dynamics for a random superposition of waves.

The EOFs of the covariance matrix calculated with the assumption that u and v are independent scalars make clear the different magnitudes of the velocity components (Fig. 4) and that only a very small correlation between the velocity components exists. The first EOFV (Fig. 8a) is predominantly a zonal velocity mode; the meridional component contains only about 3% of the total variance or energy; this lies inside the error bars and is therefore statistically not significantly different from zero. The second EOFV is mainly the meridional component. The first and second EOFV together describe a northeastward flow with a vertical structure very similar to that of the first EOF's (Fig. 5) that demand a unidirectional flow. Together, however, they contain only about the same amount of the variance as just the first EOFV of the velocity dot-product matrix (Fig. 5a). In Fig. 8c,d the EOFEs calculated with u and v as independent quantities show clearly that the velocity components are strongly uncorrelated. The first and the second EOFEs are almost zonal velocity modes with the vertical shape of the first and second EOFE describing the unidirectional flow. Finally the third EOFE (not shown, but statistically significant) describes a pure meridional velocity direction. Consequently, for the variability during LOTUS, at least twice as many u–v independent EOFs are required as in the case when the EOFs describe a unidirectional flow to represent the same fraction of en-

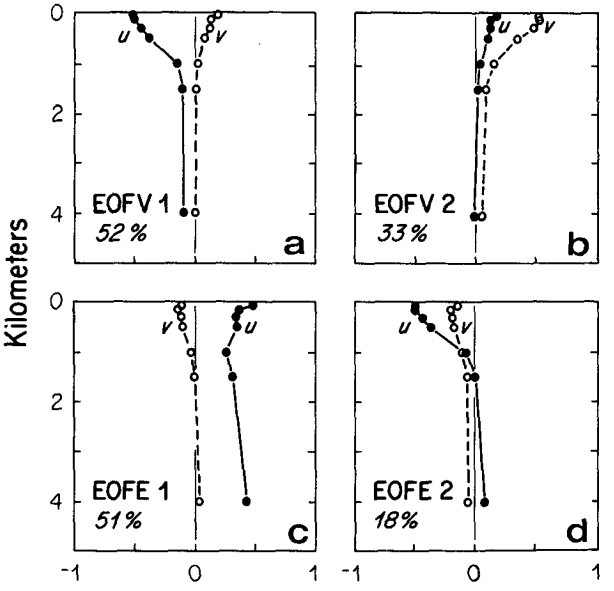

FIG. 8. First and second EOFV (a and b) and EOFE (c and d) obtained from a time-averaged covariance matrix in which the velocity components represent independent scalars.

ergy. Therefore, no large, averaged, horizontal momentum transport seems to be connected with most of the observed variability, because this would demand a strong correlation between the u and v motions.

The correlation of the velocity components with the temperature field is expressed in the EOFEs of the u, v, T-covariance matrix (Fig. 9), in which the T component has been scaled by $N/(dT/dz)$ at each depth. The temperature is almost uncorrelated with the velocity components, as indicated by the resulting independent modes for the three components u, v and T. The first EOFE, containing 58% of the total energy, is predominantly (97%) a temperature mode. The second and third EOFE describe, respectively, primarily a zonal (73% of the second EOFE) or meridional (68% of the third EOFE) flow. The differences between EOFEs and EOFVs, which obtain for the low frequency variability at LOTUS due to bottom intensification of the zonal velocity component, are not available in this case because we could not incorporate the values at 4000 m due to the lack of temperature data at this depth.

The best representation (i.e., simplest, most of the variance described) for the low-frequency variability during LOTUS is, therefore, given by an EOF describing a unidirectional, nonrotating flow; temperature and velocity are in quadrature, which suggests quasi-geostrophic dynamics. Since u and v are uncorrelated, a stochastic wave field is indicated rather than single-wave dynamics.

Our results are therefore at least qualitatively in good agreement with those of LDE (Owens 1985). The differences lie mostly in the vertical structure at the two different locations, and in the fact that at LDE small correlations between the velocity components and between the temperature and velocity seem to occur.

The EOFs resulting from the time-averaged covariance matrix are dominated by the characteristics of the most energetic motions. Since at LOTUS the energy is concentrated at very long periods, the EOFs presented above do not characterize the motions at shorter periods. In addition there could be frequency ranges in which significant heat transports and/or momentum transports occur. We therefore present in addition the

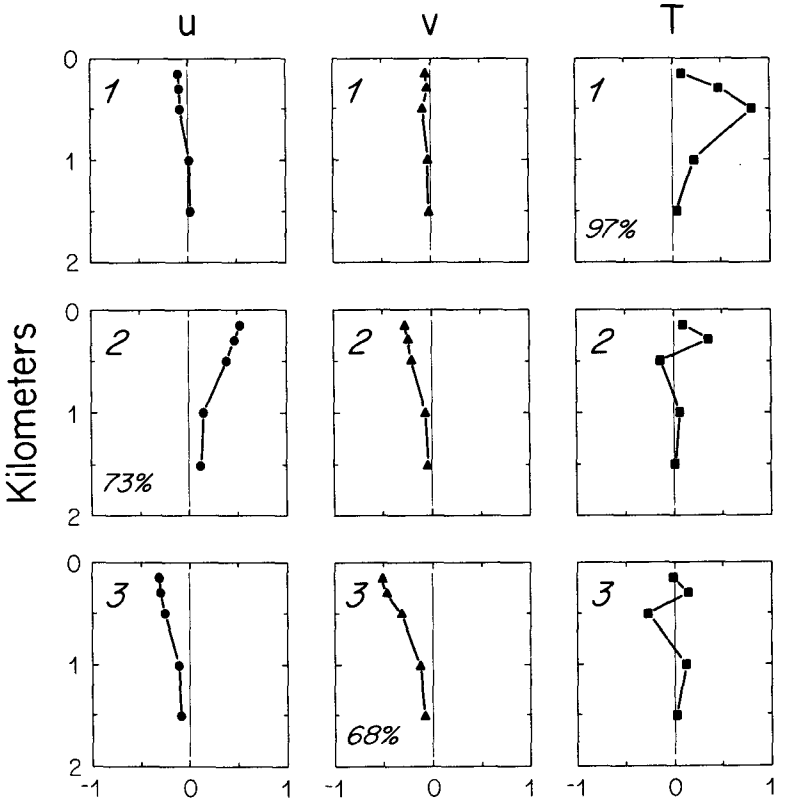

FIG. 9. First, second and third EOFE resulting from a time-averaged covariance matrix in which u, v and T are independent scalars. Here, T has been scaled by $N/(dT/dz)$ at each depth. The contribution of each EOFE (i.e., all three components taken together) to the total energy is 76%, 10%, and 7%, for the first, second, and third EOFEs, respectively. The dominating component for each EOFE has its relative contribution shown as a percentage in the figure. The temperature component of the first EOFE, for example, contains $76 \times 97 = 74\%$ of the total variance in the dataset.

EOFs for the 4 frequency ranges defined above in section 1 and Fig. 3.

Shown in Fig. 10 are the first and second EOFEs of the velocity dot-product matrix for the four frequency ranges. The first EOFE shows a strong increase of the surface intensification with increasing frequency. The period range between 10 and 30 days (called s here) is considered typical for topographic quasi-geostrophic waves (Rhines 1970; Thompson and Luyten 1976; Csanady 1988); the EOFEs show their strongest bottom intensification in this range. However, we should note that the first EOFE in this period range contains less energy than the first EOFEs of the lower period ranges, and the second EOFE for periods between 10 and 30 days has no bottom intensification.

The temperature fluxes described by the EOF analyses are small [10^{-3} to 10^{-1} (cm s^{-1})°C], are maximum at about 500 m depth, and are about the same size in the low, medium, and special frequency ranges; in the high-frequency range the temperature flux from the EOFs is even smaller. In the medium frequency range, the meridional temperature flux is 2 to 3 times larger than the zonal flux; in the low and special frequency ranges it is mainly a southeast temperature flux.

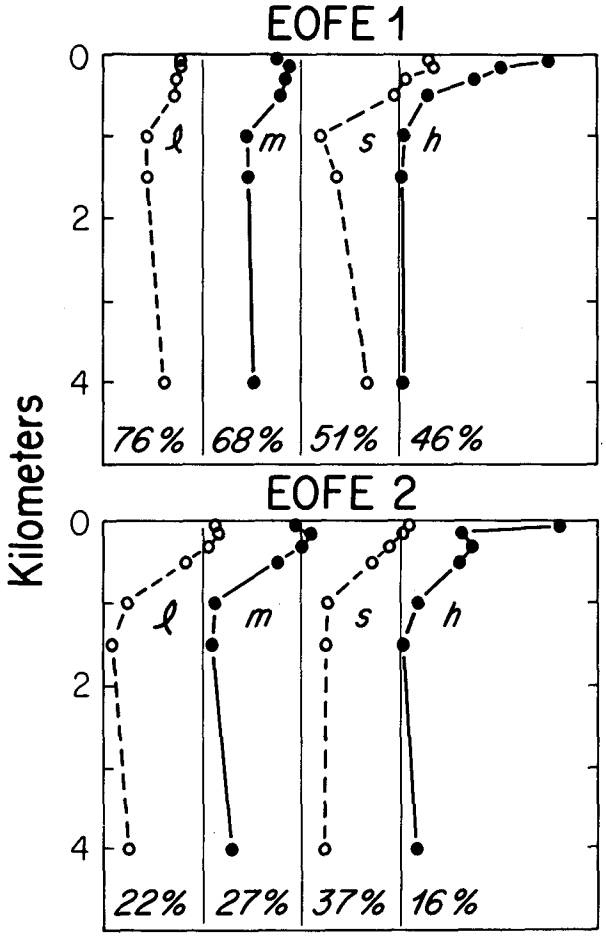

FIG. 10. First EOFE (upper panel) and second EOFE (lower panel) in 4 different frequency ranges. The letters correspond to low-frequency range (ℓ), medium-frequency range (m), special-frequency range (s), and high-frequency range (h), as in Figs. 3 and 4. The origin of the zero axis for each frequency range is progressively shifted to the right, and is located to the left of each corresponding curve.

4. Summary and conclusions

We have presented a description of the low-frequency variability observed during the Long Term Upper Ocean Study, based mainly on mooring data at 34°N, 70°W in the northwestern part of the Gulf Stream recirculation region.

The variability is dominated (Fig. 4) by zonally elongated motions of the secular time scale (periods > 100 days). In contrast to the observations in other parts of the recirculation region, the shape of the spectra (Fig. 3) is strongly depth dependent. The relative importance of fluctuations of the secular scale (measured as a fraction of the total energy at each depth) increases with depth.

The vertical structure was examined by a variety of EOF analyses, of which we prefer the EOFE dot-product version (Fig. 5c,d) for its simplicity and robustness. Sixty-six percent of the observed energy can be described by an almost barotropic mode with only a slight increase at the surface and the bottom of the ocean. By including the second empirical mode, which closely resembles the first baroclinic dynamical mode, 96% of the observed energy can be accounted for. The barotropicity of the eddy variability along 70°W increases from south to north, as observed by comparing (Fig. 7) the variability observed during MODE and LDE (Owens 1985) with that at LOTUS. However, with increasing frequency (Fig. 10) the motions at LOTUS become more and more baroclinic and surface intensified; LOTUS, of all the recirculation region datasets, provides a unique opportunity to examine surface intensification.

It is possible to diagnose aspects of the dynamics of the observations without incorporating information about the horizontal scales if one uses the information from the cross spectra in addition to the power spectra. Part of the information from the cross spectra was included in the EOFs. The best representation of the observed energy was given by an EOF that described a unidirectional nonrotating (with depth) flow; this is consistent with but does not prove linear wave dynamics. However, we emphasize strongly that u and v are uncorrelated, which demands a stochastic wave field rather than single-wave dynamics.

We note that resonant barotropic Rossby waves are predicted by linear theory to have periods of the order of one to ten days (Willebrand et al. 1980), and linear baroclinic Rossby waves only occur at periods larger than their critical period (which is 182 days at the LOTUS mooring site). Therefore, no purely linear theory can explain our observed motions whose vertical

structure is a combination of the barotropic and first baroclinic mode at lower frequencies but changes to a more baroclinic shape at higher frequencies. This suggests that the barotropic and first baroclinic mode are strongly coupled as well as having the same time scales. We would have gotten the same result from a decomposition of the time series into the dynamical modes followed by a spectral analysis, by which method Richman et al. (1977) obtained the result that the motions in the MODE region are not simply linear.

Our summary statement from this study about the dynamics of the variability during LOTUS is that the observed fluctuations are consistent with a stochastic, quasi-geostrophic wave field that may be affected by a mean current. We have no criterion to distinguish between a linear quasi-geostrophic wave field and a broad wavenumber band of Rossby waves that interact in a weakly nonlinear way, if both are affected by a mean current. Others are working on aspects of this (e.g., Owens 1979; Treguier and Hua 1987).

Acknowledgments. This work was supported by the Office of Naval Research under Contract N00014-84-C-0134, NR 083-400. We thank Ellyn T. Montgomery for initial editing of the paper, M. Ross Vennell for critically reading portions of it, and Barbara Gaffron for preparation of the manuscript.

REFERENCES

Briscoe, M. G., and R. A. Weller, 1984: Preliminary results from the Long-Term Upper-Ocean Study (LOTUS). *Dyn. Atmos. Oceans,* **8,** 243–265.

Csanady, G. T., 1988: Radiation of topographic waves from Gulf Stream meanders. *Cont. Shelf Res.,* **8,** 673–686.

Davis, R. E., 1975: Statistical methods. *Dynamics and the Analysis of MODE-I: Report of the MODE-I Dynamics Group.* Massachusetts Institute of Technology, 1–26.

Denbo, D. W., and J. S. Allen, 1984: Rotary empirical orthogonal function analysis of currents near the Oregon coast. *J. Phys. Oceanogr.,* **14,** 35–46.

Deser, C., R. A. Weller and M. G. Briscoe, 1983: Long Term Upper Ocean Study (LOTUS) at 34N, and 70W: Meteorological sensors, data, and heat fluxes for May–October 1982 (LOTUS-3 and LOTUS-4). Woods Hole Oceanogr. Inst. Tech. Rep. WHOI-83-32, 68 pp.

Fu, L.-L., T. Keffer, P. P. Niiler and C. Wunsch, 1982: Observations of the mesoscale variability in the western North Atlantic: A comparative study. *J. Mar. Res.,* **40,** 809–848.

Hardy, D. M., 1977: Empirical eigenvector analysis of vector observations. *Geophys. Res. Lett.,* **4,** 319–320.

——, and J. J. Walton, 1978: Principal components analysis of vector wind measurements. *J. Appl. Meteor.,* **17,** 1153–1162.

Hogg, N. G., 1985: Evidence for baroclinic instability in the Gulf Stream recirculation. *Progress in Oceanography,* Vol. 14, Pergamon, 209–229.

Klink, J. M., 1985: EOF Analysis of the central Drake Passage currents from DRAKE 79. *J. Phys. Oceanogr.,* **15,** 288–298.

Kundu, P. K., and J. S. Allen, 1976: Some three-dimensional characteristics of low-frequency current fluctuations near the coast of Oregon. *J. Phys. Oceanogr.,* **6,** 181–199.

——, —— and R. L. Smith, 1975: Modal decomposition of the velocity field near the Oregon coast. *J. Phys. Oceanogr.,* **5,** 683–704.

Legler, D. M., 1983: Empirical orthogonal function analysis of wind vectors over the tropical Pacific region. *Bull. Amer. Meteor. Soc.,* **64,** 234–241.

Levitus, S., 1982: Climatological Atlas of the World Ocean. NOAA Prof. Paper 13. U.S. Department of Commerce, National Oceanic and Atmospheric Administration, 173 pp.

Lippert, A., 1986: Erzeugung niederfrequenter ozeanischer Variabilitat durch fluktuierende Windfelder. Ph.D. thesis, Dept. of Theoretical Oceanography, Institut für Meereskunde Kiel, *IFM Berichte No. 150.* 135 pp.

——, and R. H. Kase, 1985: Stochastic wind forcing of baroclinic Rossby waves in the presence of a meridional boundary. *J. Phys. Oceanogr.,* **15,** 184–194.

Luyten, J. R., 1977: Scales of motion in the deep Gulf Stream and across the continental rise. *J. Mar. Res.,* **35,** 49–74.

McWilliams, J. C., and the LDE Group, 1983: The local dynamics of eddies in the western North Atlantic. Chapter 5, *Eddies in Marine Science,* A. R. Robinson, Ed., Springer-Verlag, 92–113.

——, W. B. Owens and B.-L. Hua, 1986: An objective analysis of the POLYMODE Local Dynamics Experiment I. General formalism and statistical model selection. *J. Phys. Oceanogr.,* **16,** 483–504.

Mills, C. A., S. A. Tarbell and R. E. Payne, 1981: A compilation of moored instrument data and associated hydrographic observations, Vol. XXVIII (POLYMODE Local Dynamics Experiment, 1978–1979). Woods Hole Oceanogr. Inst. Tech. Rep. WHOI-81-73, 50 pp. + 3 microfiche.

MODE Group, The, 1978: The Mid-Ocean Dynamics Experiment. *Deep-Sea Res.,* **25,** 859–910.

Montgomery, E. T., N. J. Pennington and M. G. Briscoe, 1984a: The Long Term Upper Ocean Study, cruise summary and hydrographic data report, Oceanus 141, October 1983 and Oceanus 145, January 1984. Woods Hole Oceanogr. Inst. Tech. Rep. WHOI-84-26, 70 pp.

——, —— and ——, 1984b: The Long Term Upper Ocean Study, cruise summary and hydrographic data report, Oceanus 154, May 1984. Woods Hole Oceanogr. Inst. Tech. Rep. WHOI-84-39, 44 pp.

Moore, D., 1974: Empirical orthogonal functions—A nonstatistical view. *MODE Hot Line News,* No. 67, Woods Hole Oceanographic Institution, Woods Hole, Massachusetts.

Müller, P., and C. Frankignoul, 1981: Direct atmospheric forcing of geostrophic eddies. *J. Phys. Oceanogr.,* **11,** 287–308.

Owens, W. B., 1979: Simulated dynamic balances for mid-ocean mesoscale eddies. *J. Phys. Oceanogr.,* **9,** 337–359.

——, 1985: A statistical description of the vertical and horizontal structure on the edge of the Gulf Stream recirculation. *J. Phys. Oceanogr.,* **15,** 195–205.

——, J. R. Luyten and H. L. Bryden, 1982: Moored velocity measurements on the edge of the Gulf-Stream recirculation. *J. Mar. Res.,* **40**(Suppl.), 509–524.

Price, J. F., R. A. Weller and R. R. Schudlich, 1987: Wind-driven ocean currents and Ekman transport. *Science,* **238,** 1534–1538.

Rhines, P. B., 1970: Edge-, bottom-, and Rossby waves in a rotating stratified fluid. *Geophys. Fluid Dyn.,* **1,** 273–302.

——, 1975: Waves and turbulence on a beta-plane. *J. Fluid Mech.,* **59,** 417–443.

——, 1977: The dynamics of unsteady currents. *The Sea,* Vol. VI, E. D. Goldberg, Ed., Wiley and Sons, 189–318.

Richardson, P. L., 1983: Eddy kinetic energy in the North Atlantic from surface drifters. *J. Geophys. Res.,* **88,** 4355–4367.

Richman, J. G., C. Wunsch and N. G. Hogg, 1977: Space and time scales and mesoscale motion in the sea. *Rev. Geophys. Space Phys.,* **15,** 385–420.

Schmitz, W. J., Jr., 1974: Observations of low-frequency current fluctuations on the Continental Slope and Rise near Site D. *J. Mar. Res.,* **32,** 233–251.

——, 1976: Eddy kinetic energy in the deep western North Atlantic. *J. Geophys. Res.,* **81,** 4981–4982.

——, 1978: Observations of the vertical distribution of low frequency kinetic energy in the western North Atlantic. *J. Mar. Res.,* **36,** 295–310.

——, 1984: Abyssal eddy kinetic energy in the North Atlantic. *J. Mar. Res.*, **42,** 509–536.

——, W. R. Holland and J. F. Price, 1983: Midlatitude mesoscale variability. *Rev. Geophys. Space Phys.*, **21,** 1109–1119.

Tarbell, S. A., N. J. Pennington and M. G. Briscoe, 1984: A compilation of moored current meter and wind recorder data. Vol. XXXV, Long-Term Upper Ocean Study, Moorings 764, 765, 766, 767, 770) May 1982–April 1983. Woods Hole Oceanogr. Inst. Tech. Rep. WHOI-84-36, 154 pp.

——, E. T. Montgomery and M. G. Briscoe, 1985: A compilation of moored current meter and wind recorder data. Vol. XXXVIII, Long-Term Upper Ocean Study, Moorings 787, 788, 789, 790, 792) April 1983–May 1984. Woods Hole Oceanogr. Inst. Tech. Rep. WHOI-85-39, 162 pp.

Thompson, R. O. R. Y., and J. R. Luyten, 1976: Evidence for bottom-trapped topographic Rossby waves from single moorings. *Deep-Sea Res.*, **23,** 629–635.

Trask, R. P., M. G. Briscoe and N. J. Pennington, 1982: Long Term Upper Ocean Study, a summary of historical data and engineering test data. Woods Hole Oceanogr. Inst. Tech. Rep. WHOI-82-53, 107 pp.

——, and ——, 1983a: The Long Term Upper Ocean Study, cruise summary and hydrographic data report, Oceanus 119, May 1982. Woods Hole Oceanogr. Inst. Tech. Rep. WHOI-83-7, 42 pp.

——, and ——, 1983b: The Long Term Upper Ocean Study, cruise summary and hydrographic data report, Oceanus 129, October 1982. Woods Hole Oceanogr. Inst. Tech. Rep. WHOI-83-29, 49 pp.

——, and ——, 1983c: The Long Term Upper Ocean Study, cruise summary and hydrographic data report, Endeavor 97, April 1983. Woods Hole Oceanogr. Inst. Tech. Rep. WHOI-83-33, 46 pp.

Treguier, A. M., and B. L. Hua, 1987: Oceanic quasi-geostrophic turbulence forced by stochastic wind fluctuations. *J. Phys. Oceanogr.*, **17,** 397–411.

Wallace, J. M., and R. E. Dickinson, 1972: Empirical orthogonal representation of time series in the frequency domain. Part 1: Theoretical considerations. *J. Appl. Meteor.*, **11,** 887–892.

Willebrand, J., 1978: Temporal and spatial scales of the wind field over the North Pacific and North Atlantic. *J. Phys. Oceanogr.*, **8,** 1080–1094.

——, S. G. H. Philander and R. C. Pacanowski, 1980: The oceanic response to large scale atmospheric disturbances. *J. Phys. Oceanogr.*, **10,** 411–429.

Wunsch, C., 1981: Low frequency variability of the sea. *Evolution of Physical Oceanogrphy, Scientific Surveys in Honor of Henry Stommel,* B. A. Warren and C. Wunsch, Eds., The MIT Press, 342–374.

Wyrtki, K., L. Magaard and J. Hager, 1976: Eddy energy in the oceans. *J. Geophys. Res.*, **81,** 2641–2646.